COMPARATIVE ANALYSIS OF SOLAR PHOTOVOLTAIC FED Z-SOURCE INVERTER BASED UPQC FOR POWER QUALITY ENHANCEMENT

Miska PRASAD[1], Ashok Kumar AKELLA[2]

This paper presents a solar photovoltaic (SPV) fed Z-source inverter (ZSI) based Unified Power Quality Conditioner (UPQC) for the alleviation of power quality events such as voltage sags and harmonics with sudden addition of a nonlinear load. A novel hybrid technique was also proposed for optimum maximum power point tracking (MPPT) with the combination of perturbation and observation (P&O) and incremental conductance (Inc) technique. The response of SPV fed ZSI-UPQC for mitigation of supply voltage sags and harmonics are investigated and compared with SPV fed voltage source inverter (VSI) based UPQC (VSI-UPQC) and SPV fed current source inverter (CSI) based UPQC (CSI-UPQC).

Keywords: Power quality, Voltage sag, Harmonics, UPQC, Photovoltaic.

NOMENCLATURE

k=Gain
V_m=Peak Amplitude of the fundamental input voltage
Ua, Ub, Uc=Unit Vector
V_{dm}=Desired load voltage magnitude
V^*_{La}, V^*_{Lb}, V^*_{Lc}=Reference load voltage
V_{Sa},V_{Sb}, V_{Sc}=Source voltage
V^*_{Cabc}=Reference compensator voltage
V_{Cabc}=Measured compensator voltage
I^*_{Sa}, I^*_{Sb}, I^*_{Sc}=Reference source current
I_{Sa}, I_{Sb}, I_{Sc}=Source current
I^*_{Ca}, I^*_{Cb}, I^*_{Cc}=Reference shunt compensator current
I_{Ca}, I_{Cb}, I_{Cc}=Measured shunt compensator output current
I_{pc}=Photovoltaic current
g_K=Solar irradiation
To=Operating temperature
Tref=Cell temperature
I_{SC}= Cell Short circuit current
I_{diode}=Diode current

[1] Research Scholar, Department of Electrical Engineering, National Institute of Technology Jamshedpur, India, e-mail: 2013pgphdee05@nitjsr.ac.in
[2] Associate Professor, National Institute of Technology Jamshedpur, India, e-mail: akakella.ee@nitjsr.ac.in

V_{pv}=Output voltage of the PV
I_{pv}= Out current of the PV
R_S=Series resistance
n=Diode identity factor
V_t= terminal voltage
C=No of cells
n_S=No of PV panels in series
n_P= No of PV panels in series
I_{dr}=Diode reverse saturation current
I_{rs}=Diode reverse current
I_{sh}=Short circuit current
a=Transformation ratio
t=time
V_S=Supply voltage
V_{inj}=Injected voltage
V_{load}=Load voltage
V_C= Capacitor voltage
I_L=Inductor current

1. Introduction

In recent years, many researchers have given their focus on voltage and current quality. Among all disturbances, the voltage sags, and voltage swells represent the most common, frequent and vintage power quality degrading factors in these days power system [1-3]. UPQC is one the key Custom Power Devices (CPDs) which can compensate voltage and current distortions simultaneously [4-6]. Generally, the UPQCs consist of VSI [7-9], CSI [10] and ZSI for the alleviation of voltage sags, swells, and harmonics. The VSI is buck (step-down) type so the maximum output voltage is limited by DC link voltage. A condition of shoot through would appear and damage the Insulated Gate Bipolar Transistor (IGBT) switches if upper and lower switches of each leg of VSI fired on at the same time. The CSI is a boost type so the voltage at output level is greater than the DC voltage level. One of the big problems in CSI is that the open circuit across DC inductor would appear and damage the IGBT switches if any instant of time at least of one upper and lower switches cannot be fired on and keep it on. The demerits of traditional converters such as VSI and CSI are discussed [11-12]. Therefore the application of ZSI based UPQC technology seems very promising. ZSI has both step-down and step-up facilities. Due to the presence of this unique character it permits converters to be worked in the shoot-through condition [13]. Unlike a VSI and CSI, the shoot-through state is not harmful and actually has been utilized in ZSI. A great amount of research has been carried out in ZSI and its topologies. Looking at the various advantages of ZSI over traditional converters it has decided

to study photovoltaic fed ZSI based UPQC (PV-ZSI-UPQC) and compare the performance with that of PV-VSI-UPQC and PV-CSI-UPQC topologies.

The fossil fuels are the main source of fulfilled worldwide energy demand, but at the same time due to increased price, environmental pollution, and global warming have made it compulsory used renewable energy sources [9]. Renewable energy such as solar photovoltaic seems to have an increasing importance because it has several advantages, such as it has no noise or moving parts, and it does not need any means of fuel [8]. It has low maintenance cost and it is environmental friendly [14]. Despite these advantages, the I-V characteristics of a PV panel are extremely nonlinear and alter with irradiation and temperature [15]. There is a solo working point called maximum power point (MPP) on the I-V curve of the PV panel. The PV panel produces its maximum output power and operates with a maximum efficiency under certain irradiance and temperature conditions. Therefore, MPPT techniques are needed to maintain an operating point of the PV panel at its MPPT [16].

In this work, a novel hybrid technique also proposed for optimum MPPT with the combination of P&O and InC techniques. The performance of PV fed UPQCs depends on the control algorithm used for reference voltage and current calculation. For the generation of a reference voltage and current signals currently large numbers of control techniques are used. The commonly adopted techniques are pq theory, synchronous reference frame (SRF) theory [1], [17-19] , Fuzzy Logic Controller [20, 21], Resistive Optimization Technique [22] and Neural Networks Technique [23]. This paper presents, a solar photo-voltaic (PV) fed impedance or Z-source inverter based Unified Power Quality Conditioner (ZSI-UPQC) for the mitigation of power quality issues namely voltage sags and harmonics and compare the results with conventional PV fed VSI based UPQC (VSI-UPQC and) and PV fed CSI based UPQC (CSI-UPQC). The Unit Vector Template (UVT) control strategy is used to control the operation of PV fed UPQCs. Extensive MATLAB/Simulink studies are performed for mitigation of short duration serious voltage sags and source current and load voltage harmonics. Based on the simulation results, the detailed comparative analysis is also done.

2. Configuration of UPQC

Fig. 1 depicts the power circuit configurations of the proposed SPV-ZSI-UPQC. The power circuit of UPQC consists of two six leg impedance source inverters joined back to back by a common dc-link produced by solar photovoltaic with low step-up converter and a UVT control. The series part of SPV fed UPQC is used to mitigate the destructive voltage disturbances namely voltage sags, swells, fluctuations. Similarly the shunt part of SPV fed UPQC eliminates harmonics and contributes reactive power compensation.

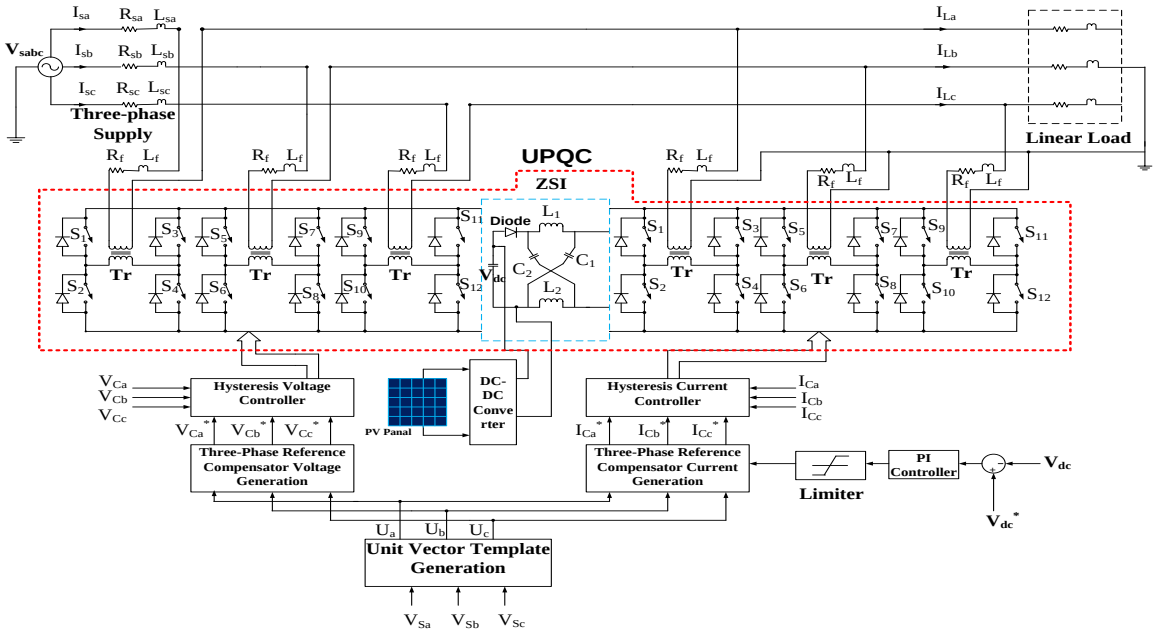

Fig. 1. Schematic diagram of SPV fed ZSI-UPQC

3. Control philosophy

The performance of PV fed UPQC system totally depends on its control technique for generation of a reference voltage and current signals. In this work UVT control technique is used to generate the reference voltage and current signals for both series and shunt active power filters.

3.1. Control technique for series active power filtar

Fig. 2 shows the Unit Vector Template (UVT) based control algorithm of series part of UPQC for the production of reference voltages. The distorted supply voltages are measured and multiplied by the gain k, which is equal to $(1/V_m)$. Where V_m is the peak amplitude of fundamental input voltage is calculated by using equation (1).

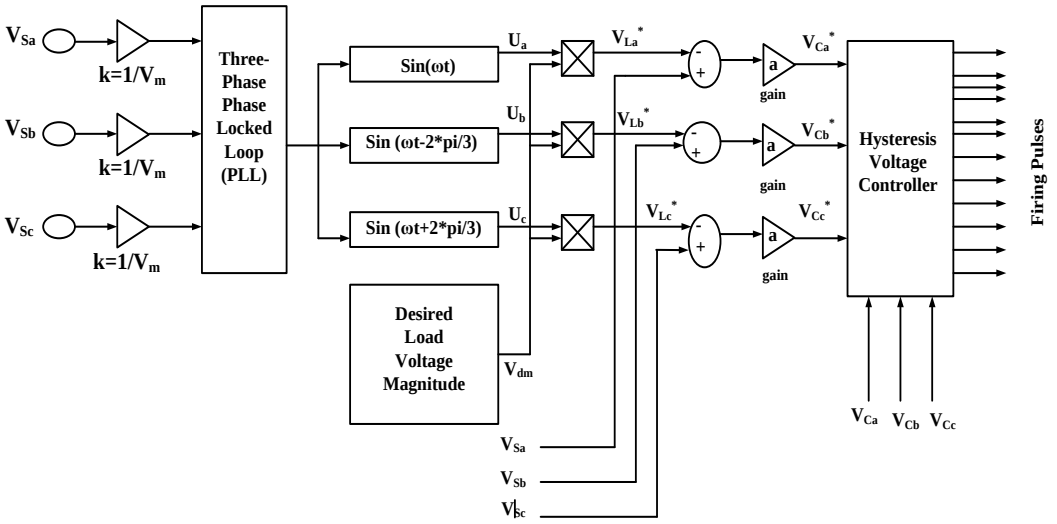

Fig. 2. UVT control technique for Series Active Power Filter

$$V_m = \sqrt{(2/3)\left(V_{Sa}^2 + V_{Sb}^2 + V_{Sc}^2\right)} \tag{1}$$

The obtained supply voltages are passed to phase locked loop (PLL). The main function of PLL is to maintain the synchronization with supply voltage and produce a unit vectors (U_a, U_b, U_c) is obtained by using equation (2).

$$\left.\begin{aligned} U_a &= Sin(\omega t) \\ U_b &= Sin(\omega t - 2\pi/3) \\ U_c &= Sin(\omega t + 2\pi/3) \end{aligned}\right\} \tag{2}$$

The reference load voltage waveforms are produced by multiplying the computed three in phase unit vector template with the desired load voltage magnitude V_{dm} is given in equation (3).

$$\begin{bmatrix} V_{La}^* \\ V_{Lb}^* \\ V_{Lc}^* \end{bmatrix} = \begin{bmatrix} V_{dm} \end{bmatrix} \begin{bmatrix} U_a \\ U_b \\ U_c \end{bmatrix} \tag{3}$$

The obtained reference load voltages ($V_{La}^*, V_{Lb}^*, V_{Lc}^*$) are compared with three-phase source voltages ($V_{Sa}, V_{Sb,} V_{Sc}$) and multiplied with ‘a’, where ‘a’ is the transformation ratio of a series transformer and produces reference compensator

voltage (V^{*}_{Cabc}). The reference compensator voltage and measured series compensator output voltage (V_{Cabc}) are then given to hysteresis voltage controller to produce the firing signals.

3.2. Control technique for shunt active power filter

The working of UVT strategy for shunt active power filter is similar to the series active power filter but in shunt active power filter additionally compares the measured dc-link voltage with reference dc-link voltage as shown in Fig. 3. The obtained error is given as input to a proportional integral controller and generates an output signal which is multiplied with UVT and produces reference source current waveforms is given in equation (4).

$$\begin{bmatrix} I^{*}_{Sa} \\ I^{*}_{Sb} \\ I^{*}_{Sc} \end{bmatrix} = [I_m] \begin{bmatrix} U_a \\ U_b \\ U_c \end{bmatrix} \tag{4}$$

The obtained reference supply current signals are compared with supply current signals and generates reference output current of shunt compensator ($I^{*}_{Ca}, I^{*}_{Cb}, I^{*}_{Cc}$) and these signals are given to hysteresis current controller along with the measured shunt-compensator output currents (I_{Ca}, I_{Cb}, I_{Cc}).

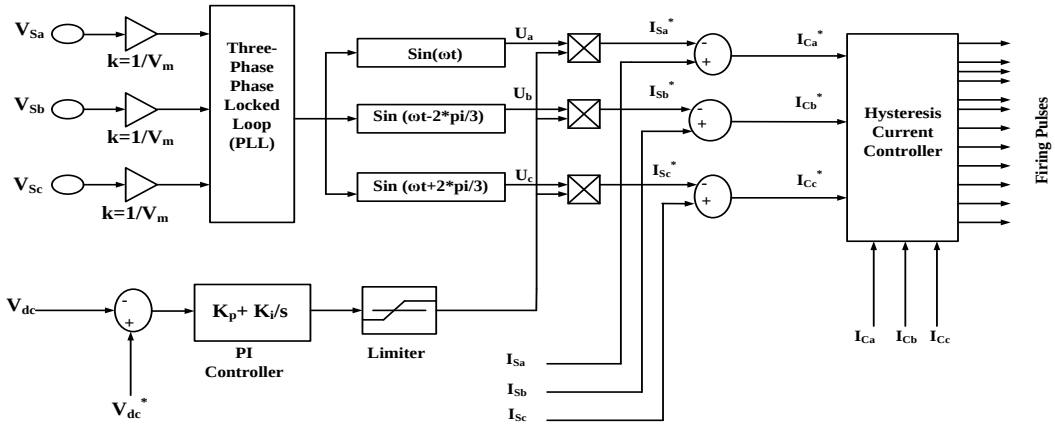

Fig. 3. UVT control technique for Shunt Active Power Filter

4. Modeling of solar photovoltaic (PV)

PV system presents an alternative solution for electricity supply especially for remote locations because of low maintenance requirement, high reliability, long

life, and stability with un-rotating units [24]. The basic diagram for modeling the solar PV system is depicted in Fig. 4.

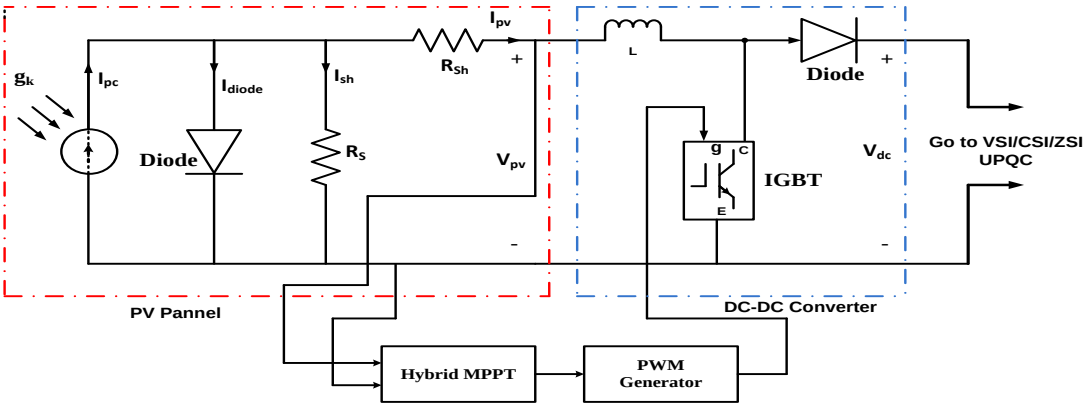

Fig. 4. PV modeling with step-up dc-dc converter and hybrid MPPT algorithm

The basic equation of the PV cell is defined in the equation (5).

$$I_{PV} = I_{pc} n_p - I_{diode} - I_{sh} \tag{5}$$

Where I_{PC} is a photocurrent mainly depends up the solar irradiation and cells working temperature, which is described in the equation (6)

$$I_{PC} = g_K \left[I_{SC} + K_i \left(T_o - T_{ref} \right) \right] \tag{6}$$

Where g_K is a solar irradiation in kW/m^2, T_o is the cell operating temperature, T_{ref} is the cell temperature at 25˚C and I_{SC} is the cells short circuit current. The current following to the diode is represented by equation (7)

$$I_{diode} = \left[e^{\left(\frac{V_{PV} + I_{PV} R_S}{n V_t C n_S} \right)} - 1 \right] I_{dr} n_P \tag{7}$$

Where I_{diode} is the diode current, V_{PV} is the output voltage of the PV panel, I_{PV} is the output current of the PV panel, R_S is the series resistance, n is the diode identity factor, V_t is the terminal voltage, C is the number of cells in PV panel, n_S is the number of PV panels in series, n_P is the number of PV panels in parallel and I_{dr} is the diode reverse saturation current. The diode reverse saturation current is defined in the equation (8).

$$I_{dr} = I_{rs}\left(\frac{T_o}{T_{ref}}\right)^3 e^{\left[\left(\frac{qE_b}{nk}\right)\left(\frac{1}{T_o}-\frac{1}{T_{ref}}\right)\right]} \tag{8}$$

Where I_{rs} is the diode reverse current at operating temperature, q is the charge of an electron, E_b is the band-gap energy of the cell and k is the Boltzmann's constant. The shunt current I_{sh} obtained from the equivalent circuit of PV module is given in the equation (9).

$$I_{sh} = \left(\frac{V_{PV} + I_{PV}R_S}{R_P}\right) \tag{9}$$

After putting the values of I_{diode} and I_{sh} from equations (7) and (9) in equation (5), we obtained equation (10).

$$I_{PV} = I_{pc}n_p - \left(e^{\left(\frac{V_{PV}+I_{PV}R_S}{nV_tCn_S}\right)} - 1\right) I_{dr}n_p - \left(\frac{V_{PV} + I_{PV}R_S}{R_P}\right) \tag{10}$$

5. Maximum power point tracking (MPPT) technique

The MPPT is the heart of the solar PV system. This paper also proposed a hybrid MPPT algorithm with a combination of P&O and InC with a dc-dc converter is integrated to measure the optimum maximum power point from the solar system.

5.1 Proposed hybrid MPPT technique

Hybrid MPPT technique is proposed to eliminate the limitations of both P&O and InC techniques is highlighted in Fig. 5. The objective of this proposed technique is to obtain the combine advantages of P&O and InC techniques. This scheme is used to calculate the output power after measuring the voltage and current from the solar system. Then it compares the power with a previous value of power by finding the change in power. The proposed algorithm checks whether $\Delta I/\Delta V$ is greater than, less than or equal to $-I/V$ and gives its decision whether to increase or decrease the terminal voltage. Fig.6 highlightes the flowchart of the proposed MPPT technique.

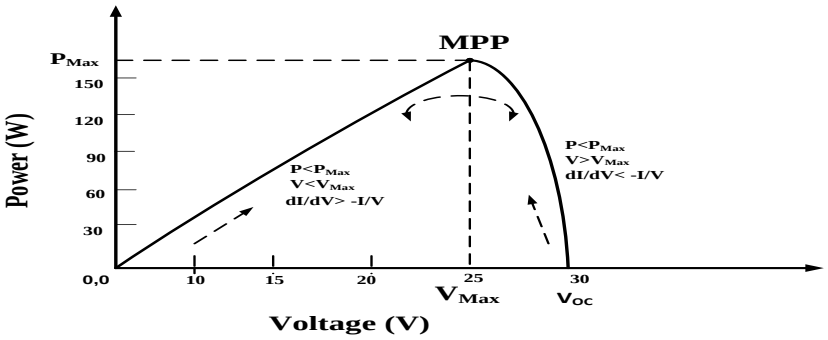

Fig. 5. Power-Voltage (P-V) characteristics of the hybrid MPPT technique

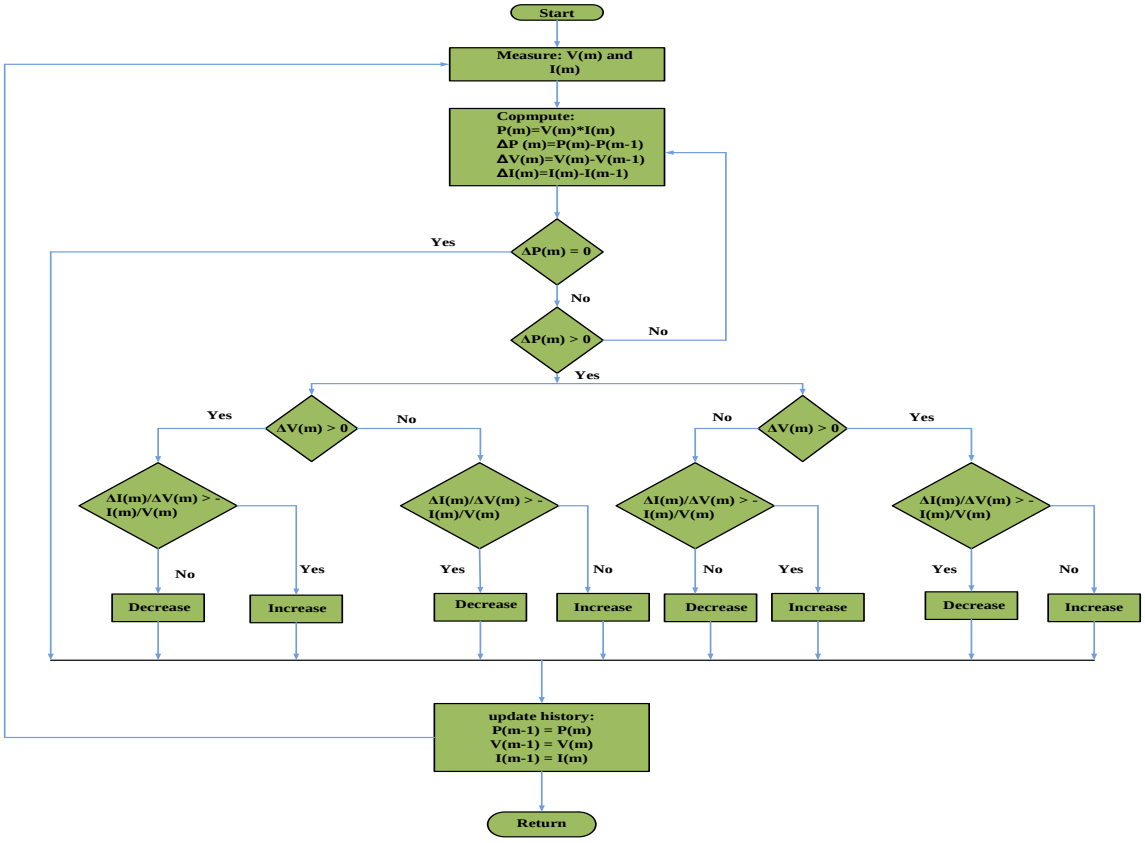

Fig. 6. Flowchart of the proposed hybrid MPPT technique

6. Simulation results and discussion

To show the effectiveness of the PV fed VSI, CSI and ZSI based UPQCs with its associated UVT control technique and the power circuit given in Fig. 1 has

been established with MATLAB/Simulink software. The simulation parameters of the system are depicted in table 1. To obtain the optimal maximum power point, the new hybrid scheme with the combination of P&O and InC technique has been used. The PV array with DC-DC converter gives greater output voltage as exposed in Fig. 7. Fig. 8(a-c) depicted that the proposed technique is more useful in extracting maximum power point (MPP =152 W) from a solar PV system compared to a maximum power point (MPP =151W) in a case of P&O technique and maximum power point (MPP=151.58 W) in a case of incremental conductance method. The most important goal of this section is to estimate the performance of the proposed PV fed ZSI-UPQC in comparison with that of traditional PV fed VSI-UPQC and CSI-UPQC for the alleviation of power quality events such as supply voltage sags and supply current as well as load voltage harmonics.

Table 1

Simulation parameters of the system

Parameters	Values
Supply Voltage (Vs)	380 V
Frequency (f)	50 Hz
Supply Resistence (Rs)	0.05 Ω
Supply Inductance (Ls)	3.5 µH
Linear Load	Active Power (P)= 5Kw Inductive reactive power (QL)= 10 kVAR
Nonlinear Load	Diode rectifier, Rd= 10Ω, Ld= 3µH
Injection Transformer	240/120 V
DC-bus Voltage (Vdc)	150 V
No of solar cells	36
Normal voltage	40 V
Normal current	4.6 A
Step-up DC-DC converter	Inductance= 0.01H
	İnput/output voltage= 40/150 V

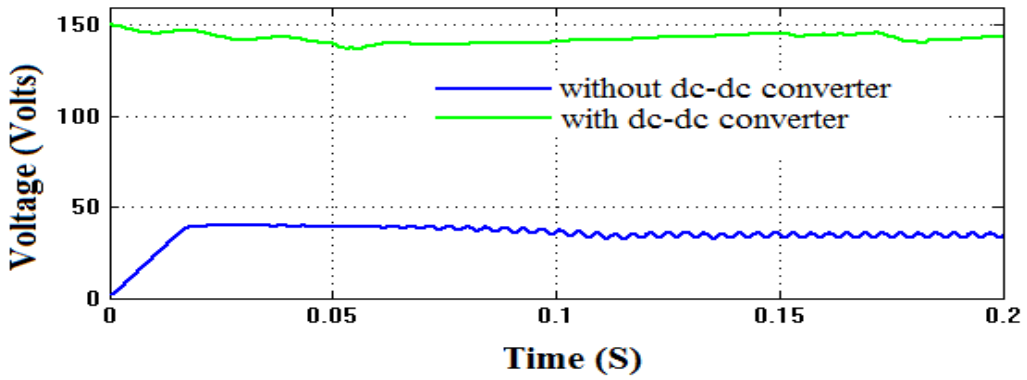

Fig. 7. PV array output voltage without DC-DC converter and with DC-DC converter

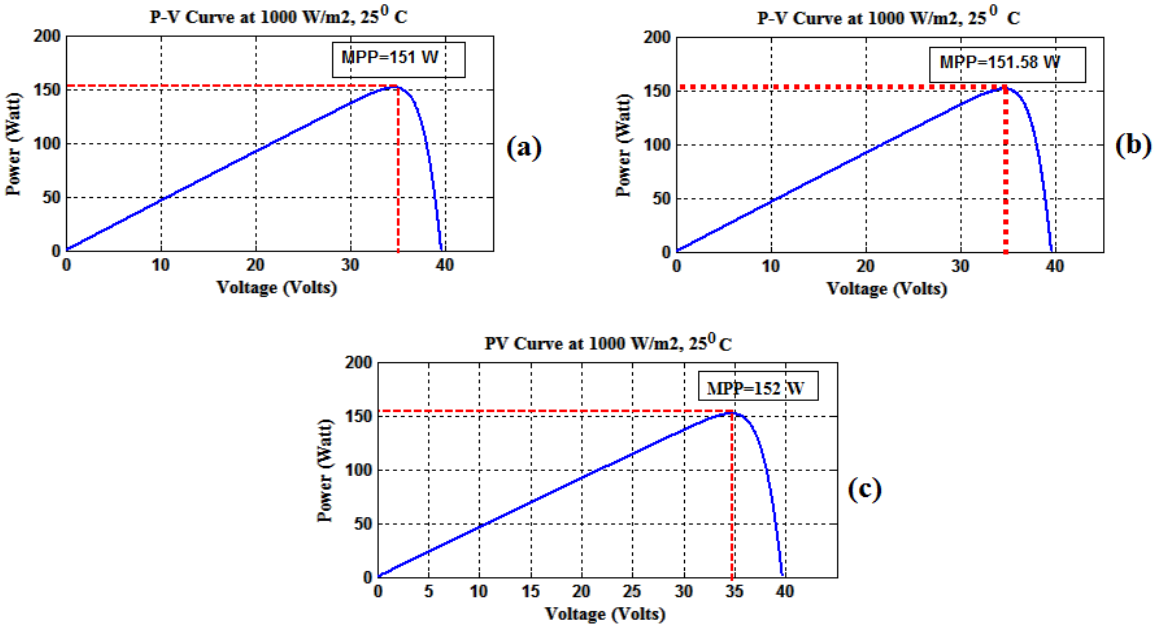

Fig. 8. Comparison of MPPT (a) Perturb and Observe (b) Incremental conductance and (c) Proposed Hybrid Technique

6.1 Performance of PV fed VSI-UPQC for mitigation of voltage sag

Due to sudden switching a nonlinear load, a three-phase voltage sag occurs in the supply terminals of the distribution network from t=0.05s to t= 0.15s for fourteen cycles of the supply voltage. For voltage sag of 15%, the supply voltage (v_S), RMS supply voltage (RMS v_S), injected voltage (V_{Inj}), load voltage (V_{Load}) and dc-link capacitor voltage (V_{dc}) are observed and depicted in Fig. 9(a-e). For a period of voltage sag only PV fed VSI-UPQC is connected to the system and provide a correct amount of missing voltage quickly as shown in Fig. 9c and minimize the effect of serious voltage sag so that load voltage become acceptable level as highlighted in Fig. 9d.

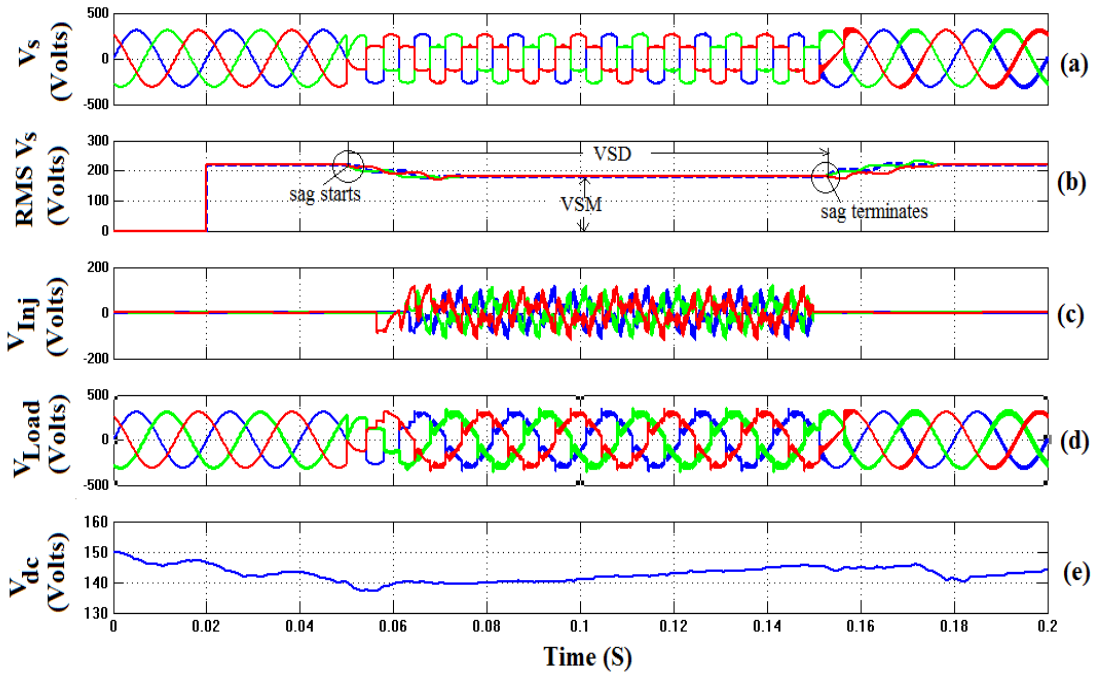

Fig. 9. Simulation results of PV fed VSI-UPQC (a) supply voltage (b) RMS supply voltage (c) Injected voltage (d) Load voltage and (e) DC-link Voltage

6.2 Performance of PV fed CSI-UPQC for mitigation of voltage sag

Fig. 10(a-e) shows the compensation effect of PV fed CSI-UPQC during voltage sag condition. For voltage sag of magnitude 15%, the supply voltage (V_S), RMS supply voltage (RMS V_S), injected voltage (V_{Inj}), load voltage (V_{Load}) and dc-link inductor current (I_{dc}) are noted and highlighted in Fig. 10(a-e). The solar PV fed CSI-UPQC comes into action for a duration of voltage sag event and produces accurate voltage magnitude with proper polarity and introduce into the distribution network. Due to this load voltage becomes insensitive to voltage sags as shown in Fig. 10d. Fig. 10e demonstrates the variation of dc-link inductor current during sudden switching a nonlinear load.

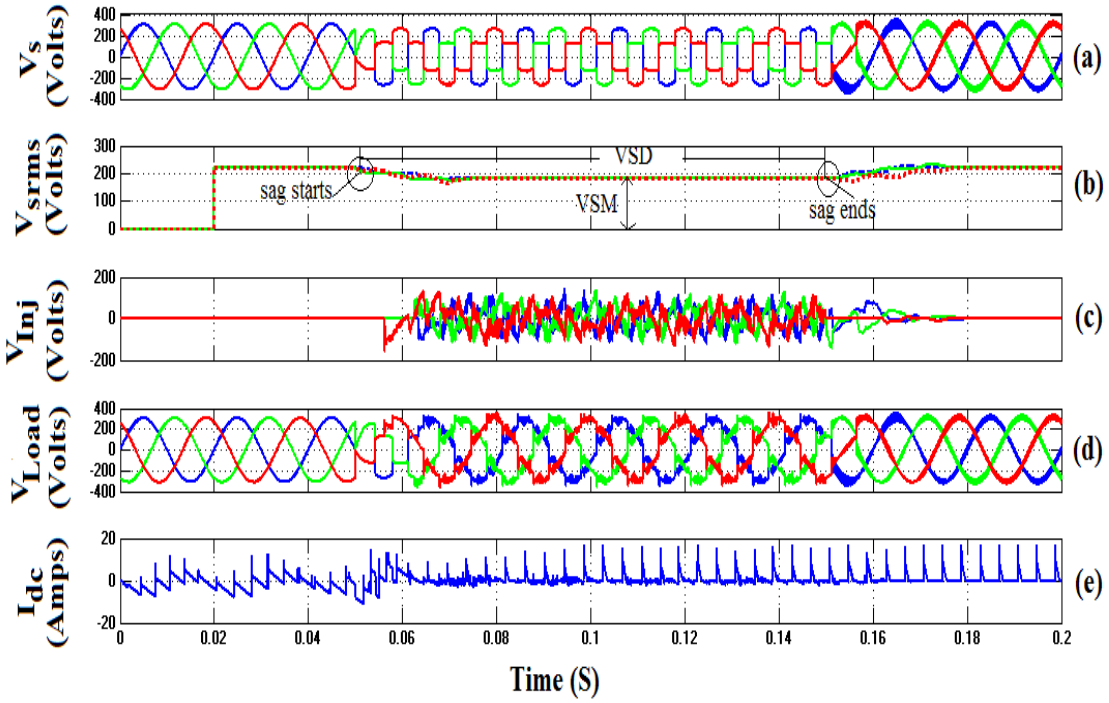

Fig. 10. Simulation results of PV fed CSI-UPQC (a) supply voltage (b) RMS supply voltage (c) Injected voltage (d) Load voltage and (e) DC-link Current

6.3 Performance of PV fed ZSI-UPQC for mitigation of voltage sag

Fig. 11(a-f) highlights the supply voltage (V_S), RMS supply voltage (RMS V_S), injected voltage (V_{Inj}), load voltage (V_{Load}), voltage across capacitor (V_C) and current in the inductor (I_L) of PV fed ZSI-UPQC during voltage sag condition. A three-phase balanced voltage sag of magnitude 15% encounters in the interval of 0.05 s $\leq$ t $\geq$ 0.15 s for fourteen cycles of the supply voltage as shown in Figs. 11a and b. During voltage sag condition source voltage decreases and at t= 0.05s to t= 0.15s the PV fed ZSI-UPQC joined to the system and produces a right magnitude of compensation voltage with correct polarity and eliminate the destructive voltage sags as shown in Fig. 11c. As a result load voltage insensitive to supply voltage disturbances as shown in Fig. 11d. The variation of capacitor voltage and inductor current of PV fed ZSI-UPQC are highlighted in Figs. 11e and f.

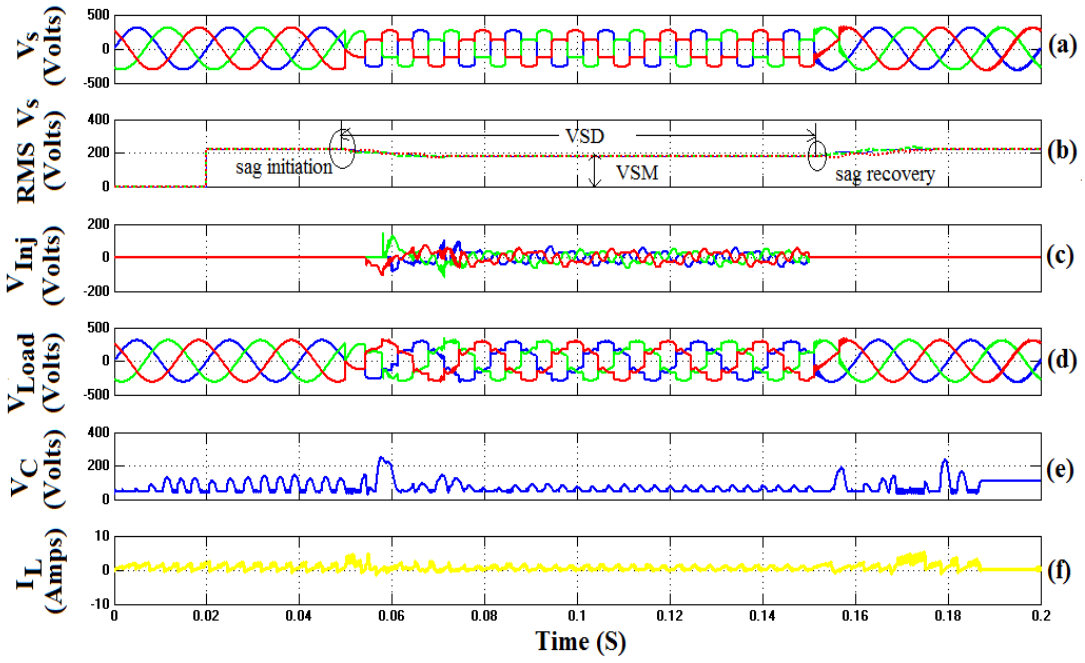

Fig. 11. Simulation results of PV fed ZSI-UPQC (a) supply voltage (b) RMS supply voltage (c) Injected voltage (d) Load voltage and (e) Capacitor voltage and (f) Inductor current

7. Comparative analysis of VSI, CSI and ZSI based UPQCs

Compensated and uncompensated load voltages under voltage sag condition are depicted in Fig. 12. Initially, PV fed VSI, CSI, and ZSI based UPQCs are not connected to the system so system experiences voltage sag of a magnitude of 15% (46.95V) of the supply voltage. During voltage sag event PV fed VSI-UPQC injects the voltage of 100 volts, CSI-UPQC injects the voltage of 134 volts and ZSI-UPQC injects the voltage of 50 volts as shown in Fig. 12a. The solar PV fed ZSI-UPQC generates the appropriate amount of injected voltage compared to VSI-UPQC and CSI-UPQC. As a result load voltage becomes sinusoidal as shown in Fig. 12b.

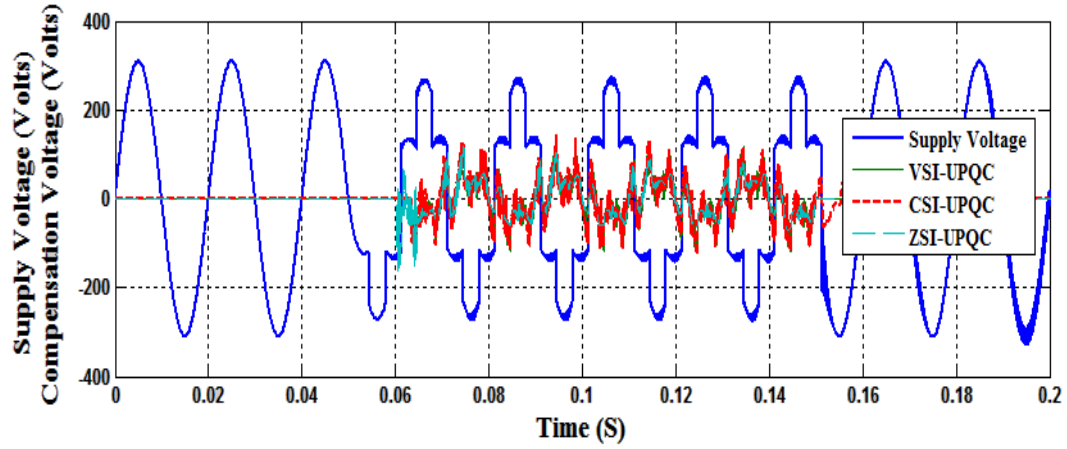

(a)

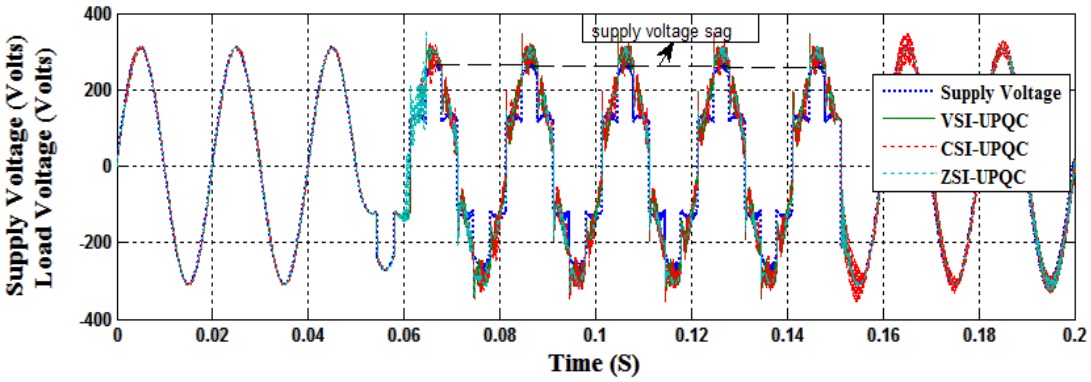

(b)

Fig. 12. Comparison of VSI, CSI and ZSI based UPQCs under voltage sag (a) Injected voltages and (b) Load voltages

The performance of load voltage and source current harmonics filtering of PV fed-UPQCs during load switching condition is illustrated in Table 2 and 3. During load switching the source current THD_i without UPQCs is obtained as 7.28%, while, THD_i of source current after compensation is found to be 1.67%, 1.66% and 160% in the case of VSI-UPQC, CSI-UPQC and ZSI-UPQC respectively as shown in Table 2. Thus, 78.02% reduction in THD_i has been achieved using ZSI-UPQC compared to 77.06% reduction in THD_i of VSI-UPQC and 77.20% reduction in THD_i of CSI-UPQC.

Table 2

Supply current harmonics THD_i of VSI, CSI and ZSI UPQCs

Without UPQCs	VSI-UPQC		CSI-UPQC		Proposed ZSI-UPQC	
	With VSI-UPQC	Improvement in THDi (%)	With CSI-UPQC	Improvement in THDi (%)	With ZSI-UPQC	Improvement in THDi (%)
7.28	1.67	77.06	1.66	77.20	1.60	78.02

The THD_v of load voltage measured without VSI, CSI, and ZSI based UPQCs is observed as 25.96%, whereas the same is observed as 1.72% in the presence of VSI-UPQC, 4.20% in the case of CSI-UPQC and 0.07% in the presence of ZSI-UPQC as shown in Table 3. Thus, 93.37%, 83.82% and 99.73% reduction in THD_v have been achieved. The ZSI-UPQC shows the superior performance of reduction in THD_v in compare to VSI-UPQC and CSI-UPQC.

Table 3

Load voltage harmonics THD_s of VSI, CSI and ZSI UPQCs

Without UPQCs	VSI-UPQC		CSI-UPQC		Proposed ZSI-UPQC	
	With VSI-UPQC	Improvement in THDs (%)	With CSI-UPQC	Improvement in THDs (%)	With ZSI-UPQC	Improvement in THDs (%)
18.62	2.31	87.60	2.48	86.68	1.48	92.05

8. Conclusions

This paper highlights, a solar photo-voltaic (PV) fed three inverter configurations of UPQC such as PV-VSI-UPQC, PV-CSI-UPQC, and PV-ZSI-UPQC for the minimization of sags and harmonics with addition of a nonlinear load. A novel hybrid method with the combination of P&O and InC technique is also proposed. The proposed technique shows the superior performance to produce maximum power output compared to P&O and InC techniques. The proposed technique also controls the power loss by controlling the oscillations around the MPP. The PV fed UPQCs is responsible for the fast and accurate production of injecting voltage and injects it into the system for compensation of supply voltage disturbances such as voltage sags. The obtained simulation results show that PV fed ZSI-UPQC injects the appropriate amount of three-phase injecting voltage compared to PV fed VSI and CSI based UPQCs. The simulation results also prove that the proposed PV fed ZSI-UPQC shows a superior capability to annihilate the source current and load voltage harmonics compared to PV fed VSI-UPQC and CSI-UPQC.

REFERENCES

[1]. *A.K. Panda, N. Patnaik*, "Management of reactive power sharing & power quality improvement with SRF-PAC based UPQC under unbalanced source voltage condition," Electrical Power and Energy Systems, **vol. 84,** 2017, pp. 182–194.

[2]. *M. P. Kazmierkowski, R. Krishnan, F. Blaabjerg,* "Control in Power electronics selected problems," Academic press, Amsterdam Bostom London, 2002, pp. 462-482.

[3]. *P.R. Babu, P. K Dash, S.K Swain, S. Sivanagaraju*, "A new fast discrete S-transform and decision tree for the classification and monitoring of power quality disturbance waveforms," International Transactions on Electrical Energy Systems, **vol.24,** 2014, pp.1279-1300.

[4]. *A. Basit, A.D. Hansen, M. Altin, P. E. Sorensen, M. Gamst*, "Compensating active power imbalances in power system with large-scale wind power penetration," Journal of Modern Power System and Clean Energy, **vol.4,** no.2, 2016, pp.229–237, 2016.

[5]. *S.K. Khadem, M. Basu, M. F. Conlon,* "A comparative analysis of placement and control of UPQC in DG integrated grid connected network," Sustainable Energy, Grids and Networks, **vol.6**, 2016, pp.46–57.

[6]. *X.U. Yunfei, X. Xiao, T. Sun, Y. Long,* "Voltage sag compensation strategy for unified power quality conditioner with simultaneous reactive power injection," International Journal of Modern Power system and Clean Energy, **vol.4**, no.1, 2016, pp.113-122, 2016.

[7]. *P. Vodapalli, T.R.S Reddy, S.T. Kalyani,* "A New Unified Power Quality Conditioner for Grid Integration of PV System and Power Quality Improvement Feature Distribution System," IEEE International Conference on Electrical, Electronics, Signals, Communication and Optimization (EESCO). 24-25 Jan. 2015.

[8]. *A.R Reisi, M. H. Moradi, H. Showkati,* "Combined photovoltaic and unified power quality controller to improve power quality," Solar Energy, **vol.88**, 2013, pp.154–162.

[9]. *Y. Pal, A. Swaroop, B. Singh,* "A comparative analysis of different magnetics supported three phase four wire unified power quality conditioners – a simulation study," Electrical Power Energy System, **vol.47**, 2013, pp.436–47.

[10]. *M.E. Pedro, J. R. Espinoza, C. R. Baier, J.I. Guzman, E.E. Espinosa,* "Unified Power Quality Conditioner based on Current Source Converters for Harmonic Mitigation using a Decoupled Control Strategy," IECON 2011 - 37th Annual Conference on IEEE Industrial Electronics Society. 7-10 Nov. 2011.

[11]. *M. Hanif, M. Basu, K. Gaughan,* "Understanding the operation of a Z-source inverter for photovoltaic application with a design example," IET Power Electron, **vol.4**, no.3, 2011, pp.278–287.

[12]. *P. Kumar, N. Kumar, A.K Akella,* "Comparative Analysis of Voltage and Current source inverter based DSTATCOM systems," Turkish Journal of Electrical Engineering and Computer sciences, **vol.24**, 2016, pp.3838-3851.

[13]. *M. Murali, P. Deshpande, B. Virpurwala, P. Bhavsar,* "Simulation and Fabrication of single phase Z-source inverter for resistive load," U.P.B. Sci. Bull., Series C, **vol.78**, no. 1, 2016, pp.112-124.

[14]. *S. Sumathi, L. A. Kumar, P. Surekha,* "Solar PV and Wind Energy Conversion Systems," Springer International Publishing Switzerland, 2015.

[15]. *Y. Bouzelata, E. Kurt, R. Chenni, N. Altın,* "Design and simulation of a unified power quality conditioner fed by solar energy," International journal of hydrogen energy, **vol.40**, no.44, , 2015, pp.15267–15277.

[16]. *S. Saravanan, N.R Babu,* "Maximum power point tracking algorithms for photovoltaic system – A review," Renewable and Sustainable Energy Reviews, **vol.57**, 2016, pp.192–204.

[17]. *N. Patnaik, A.K Panda*, "Performance analysis of a 3 phase 4 wire UPQC system based on PAC based SRF controller with real time digital simulation," Electrical Power and Energy Systems, **vol.74**, 2015, pp.212–21.

[18]. *A.J Viji, T.A.A Victoire*, "Enhanced PLL based SRF control method for UPQC with fault protection under unbalanced load conditions," Electrical Power and Energy Systems, **vol.58,** 2014, pp.319–28.

[19]. *S.D.K.Varma, Y.P. Obelesh, Ch. Saibabu,* "An Improved Synchronous Reference Frame Controller based Dynamic Voltage Restorer for Grid Connected Wind Energy System," International Journal of Renewable Energy Research, **vol.6**, no.3, 2016, pp.880-888.

[20]. *R.K Patjoshi, V.R Kolluru, K. Mahapatra,* "Power quality enhancement using fuzzy sliding mode based pulse width modulation control strategy for unified power quality conditioner," Electrical Power and Energy Systems, **vol.84,** 2017, pp.153–167.

[21]. *M.A Kouadria, T. Allaoui, M. Denai, "*Fuzzy control of a three-phase Shunt active power filter for harmonic compensation in wind-diesel standalone system," U.P.B. Sci. Bull., Series C, Vol. 78, Iss. 4, 2016, pp.70-82

[22]. *R.K Patjoshi, K. Mahapatra,* "Resistive optimization with enhanced PLL based nonlinear variable gain fuzzy hysteresis control strategy for unified power quality conditioner," Electrical Power and Energy Systems, **vol.83**, 2016, pp. 352–363.

[23]. *S. Kasa, S. Ramasamy,* "Photovoltaic fed Dynamic Voltage Restorer with Voltage Disturbance Mitigation Capability Using ANFIS Controller," International Journal of Renewable Energy Research, **vol.6,** no.3, 2016, pp.825-832, 2016.

[24]. *M. Mihai, A. Badea, R. Vidu*, "Analysis of the PV system performance through simulation: a case study," U.P.B. Sci. Bull., Series C, **vol. 78**, no. 4, 2016, pp.184-194.